Stabilization of the inorganic-organic interface

Julian Eastoe

University of BRISTOL

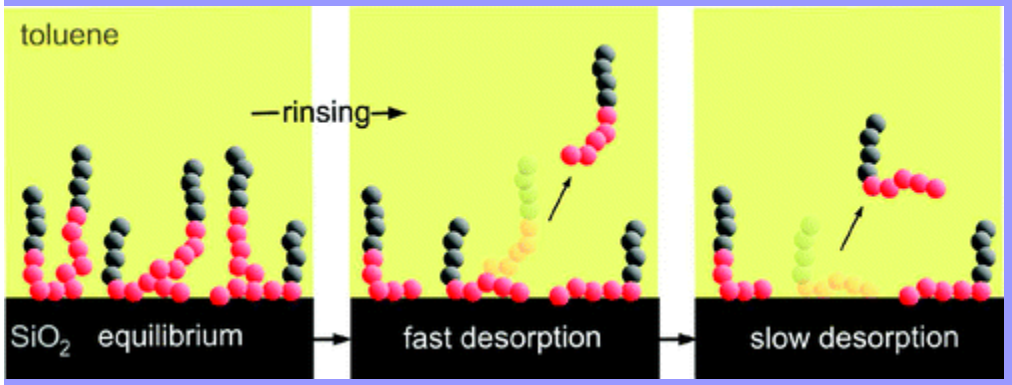

surfactant kinetics at model planar oil / SiO_2 interfaces

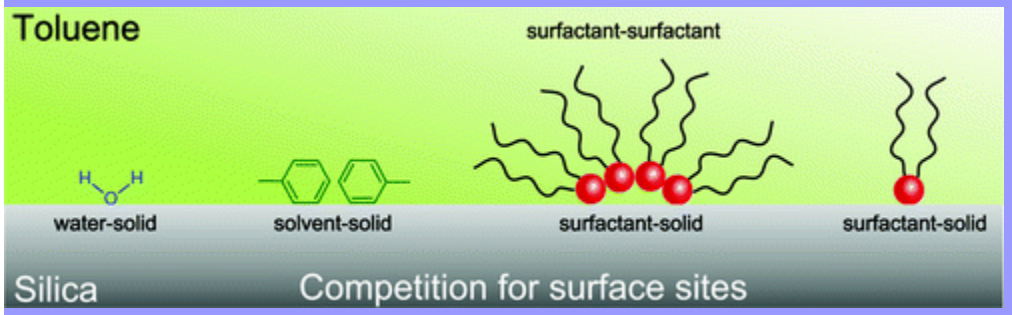

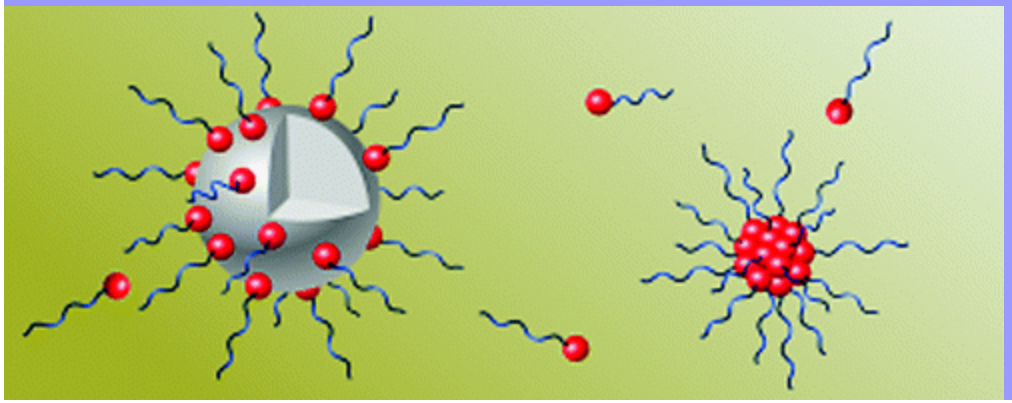

structures of colloidal dispersions

layer kinetics in colloidal dispersions

ATR-FTIR

model silicon/silica-oil interface

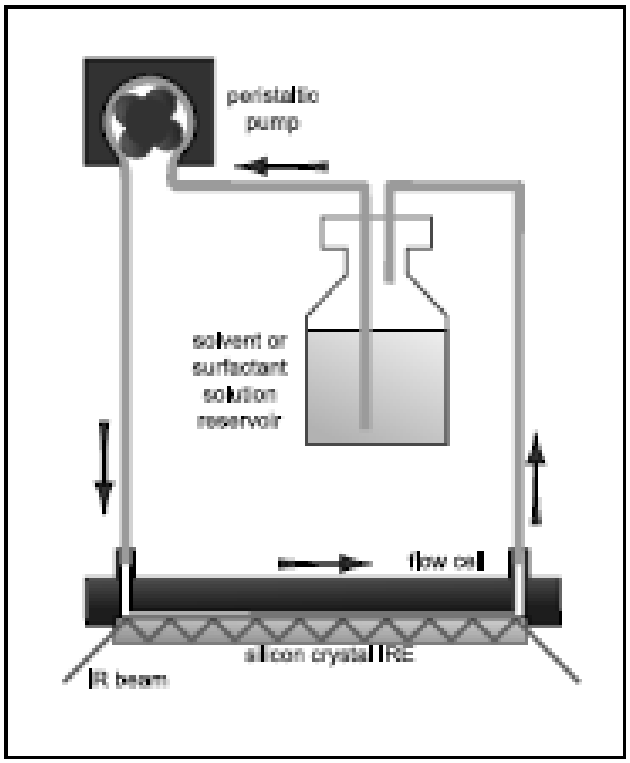

$$\Gamma = \frac{(A/N) - \epsilon C_b d_e}{1000\epsilon(2d_e/d_p)}$$

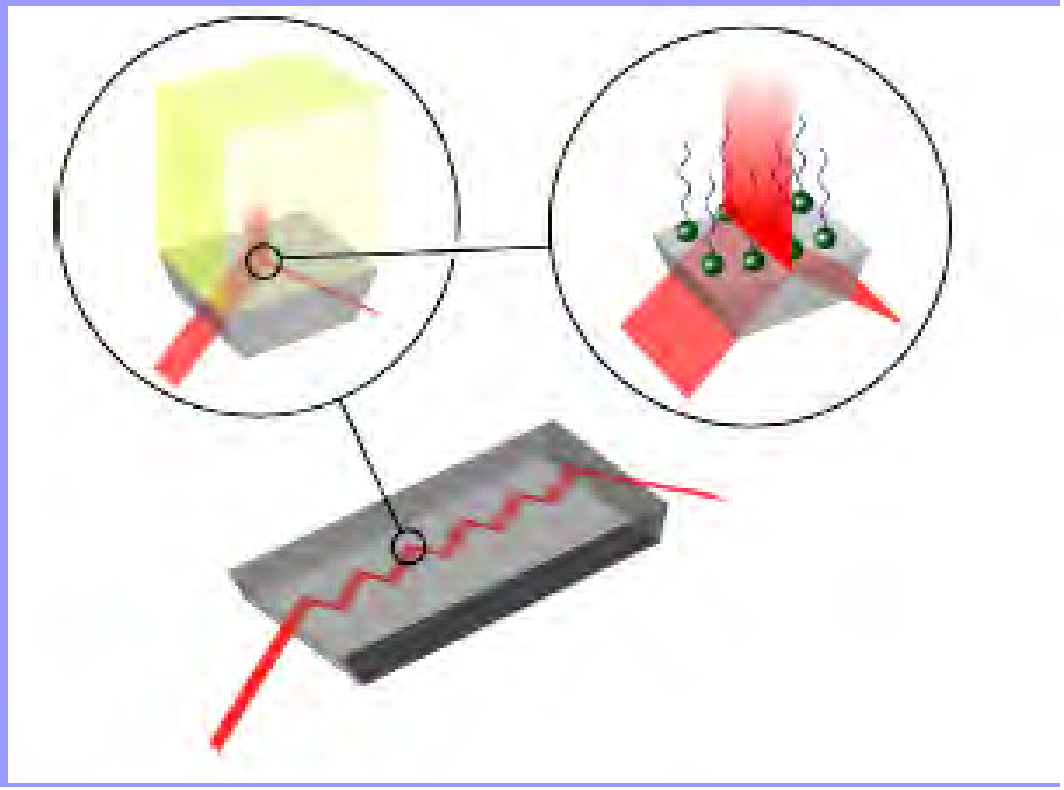

A – absorbance

N – # reflections

ε – extinction

$d_{e,p}$ – depths

adsorption

surfactants

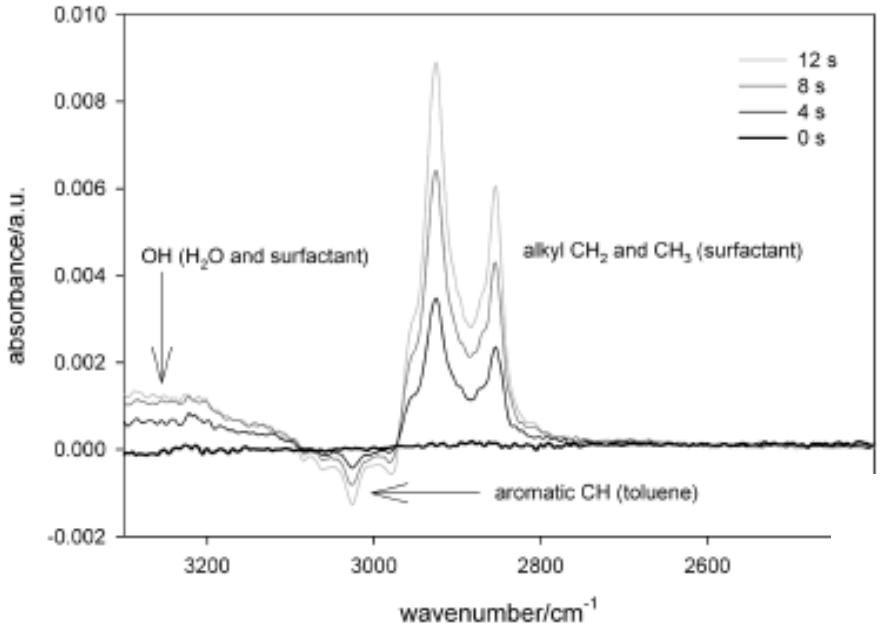

C_nE_m

$(C_nH_{2n+1})_2N(CH_3)_2Br$
n = 10, 12, 14

Adsorption and desorption of **nonionic** surfactants on silica from toluene studied by ATR-FTIR

Julian Eastoe, Rico Tabor, Peter Dowding

Langmuir 2009, 25, 9785–9791

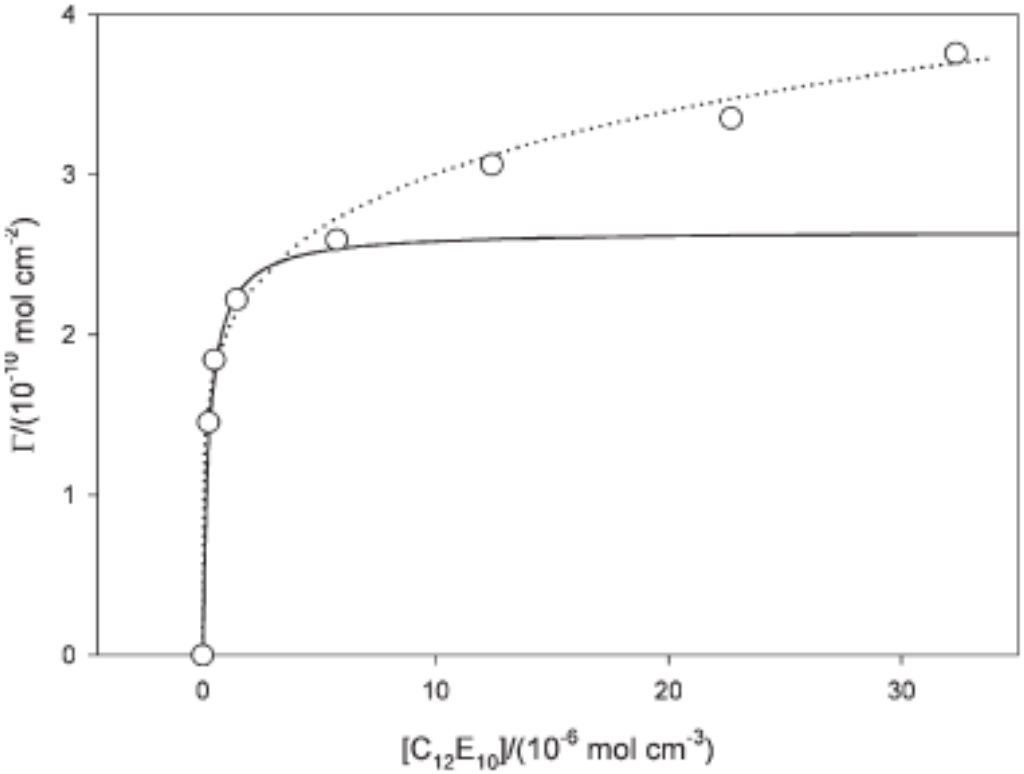

Adsorption and desorption of **cationic** surfactants onto silica from toluene studied by ATR-FTIR

Rico Tabor, Julian Eastoe*, Peter Dowding

Langmuir 2009, Accepted 28-08-09 ID: la-2009-02270e.R1

desorption

non-ionic surfactants

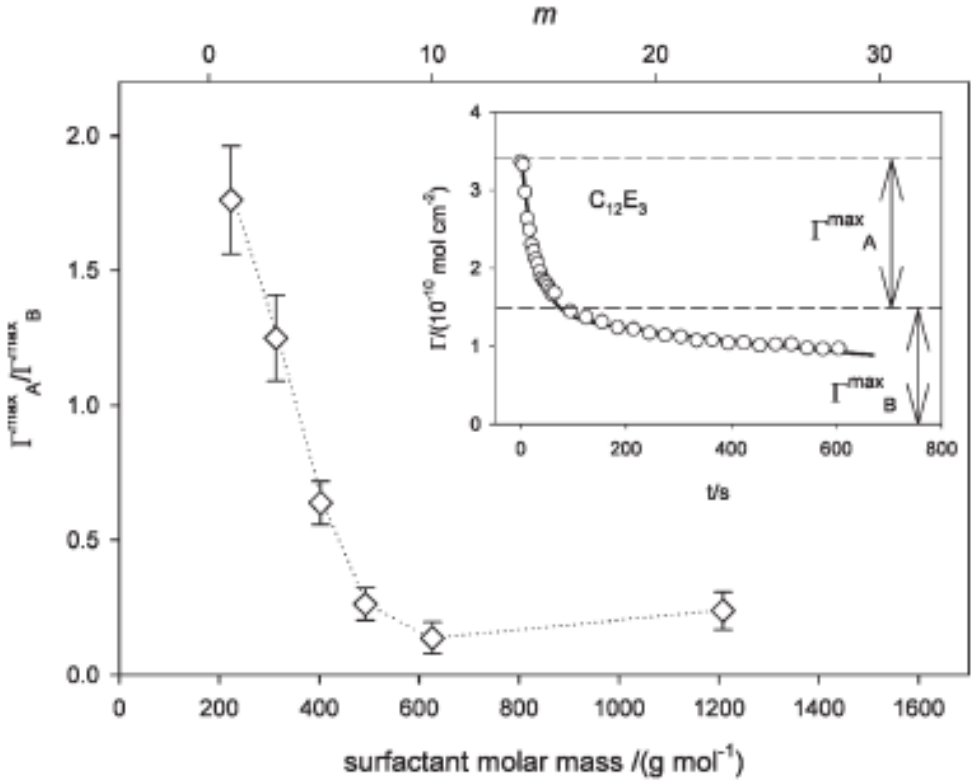

$$\Gamma_A^{max} \frac{d\theta_A}{dt} = -k_A^{des}\theta_A$$

$$\Gamma_B^{max} \frac{d\theta_B}{dt} = -k_B^{des}\theta_B$$

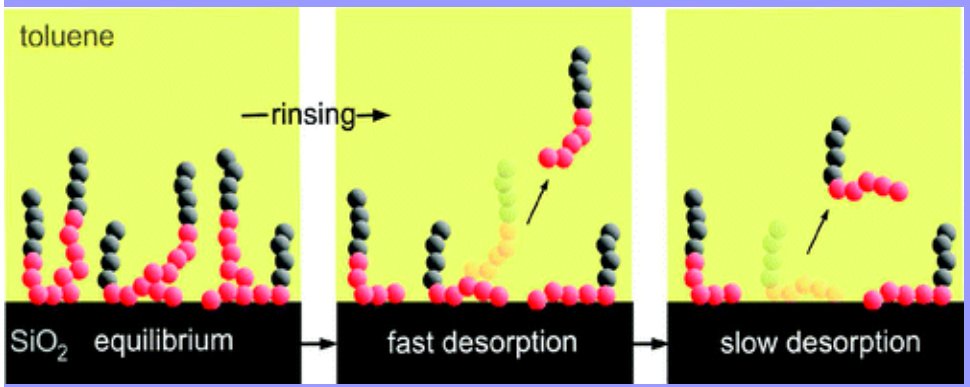

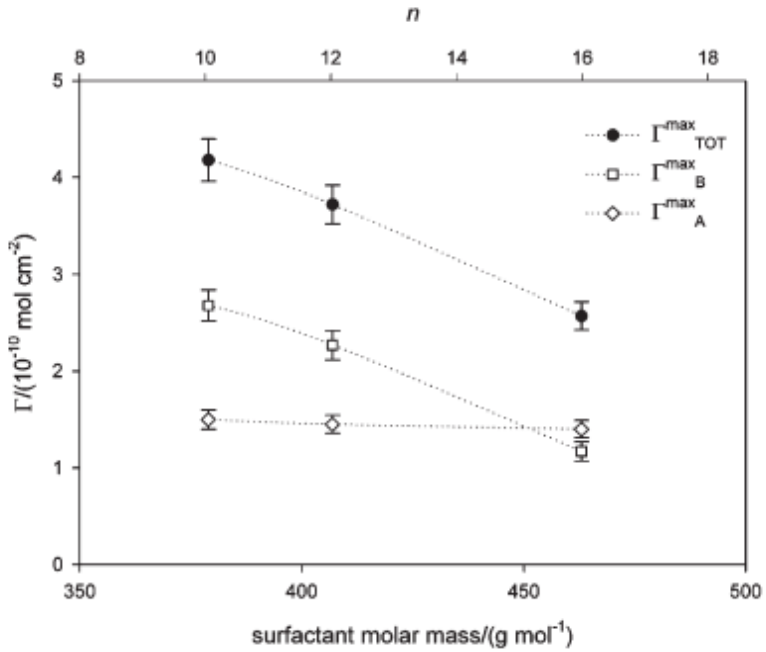

solvent comparison

di-alkyl cationic surfactants

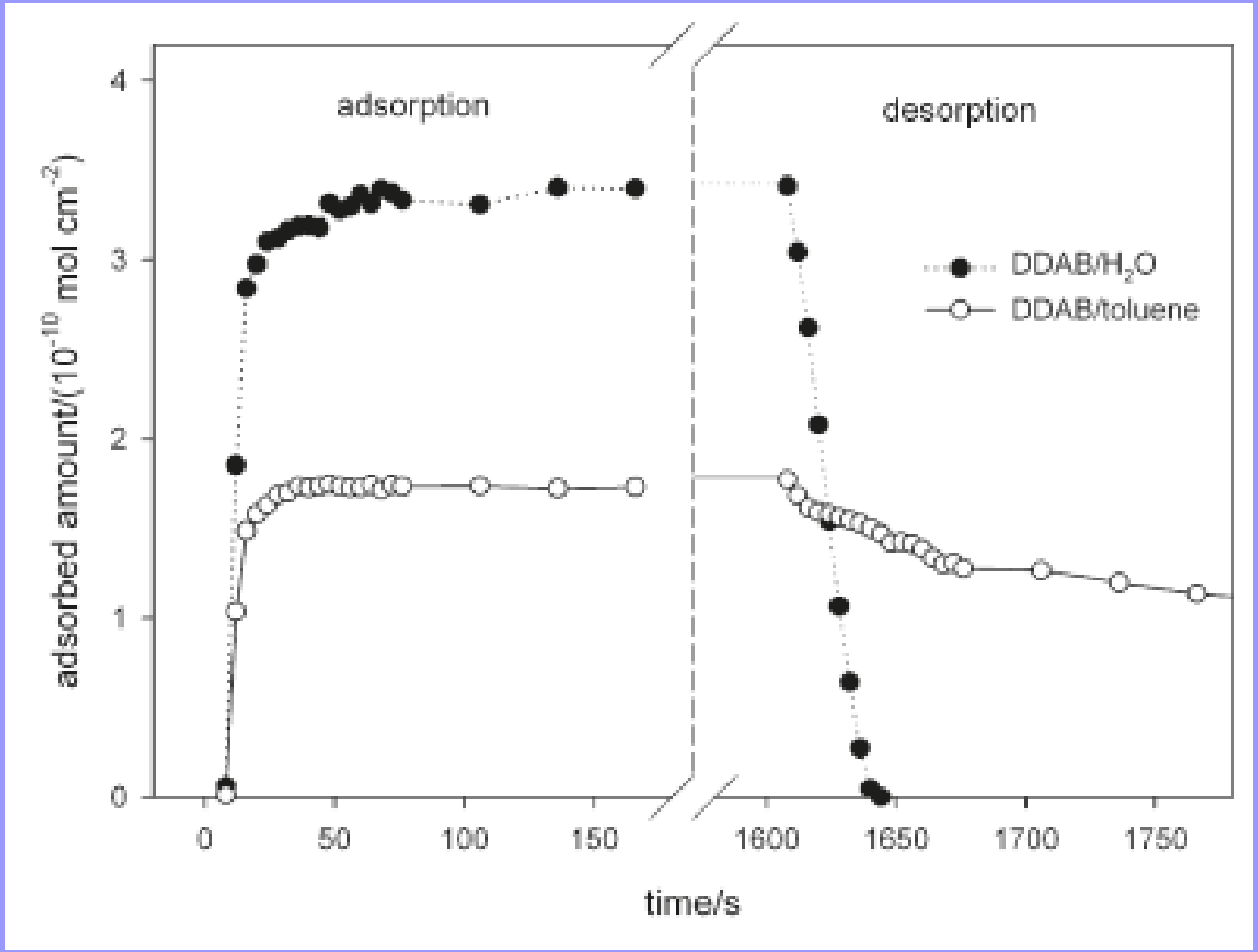

solvency

di-alkyl cationic surfactants

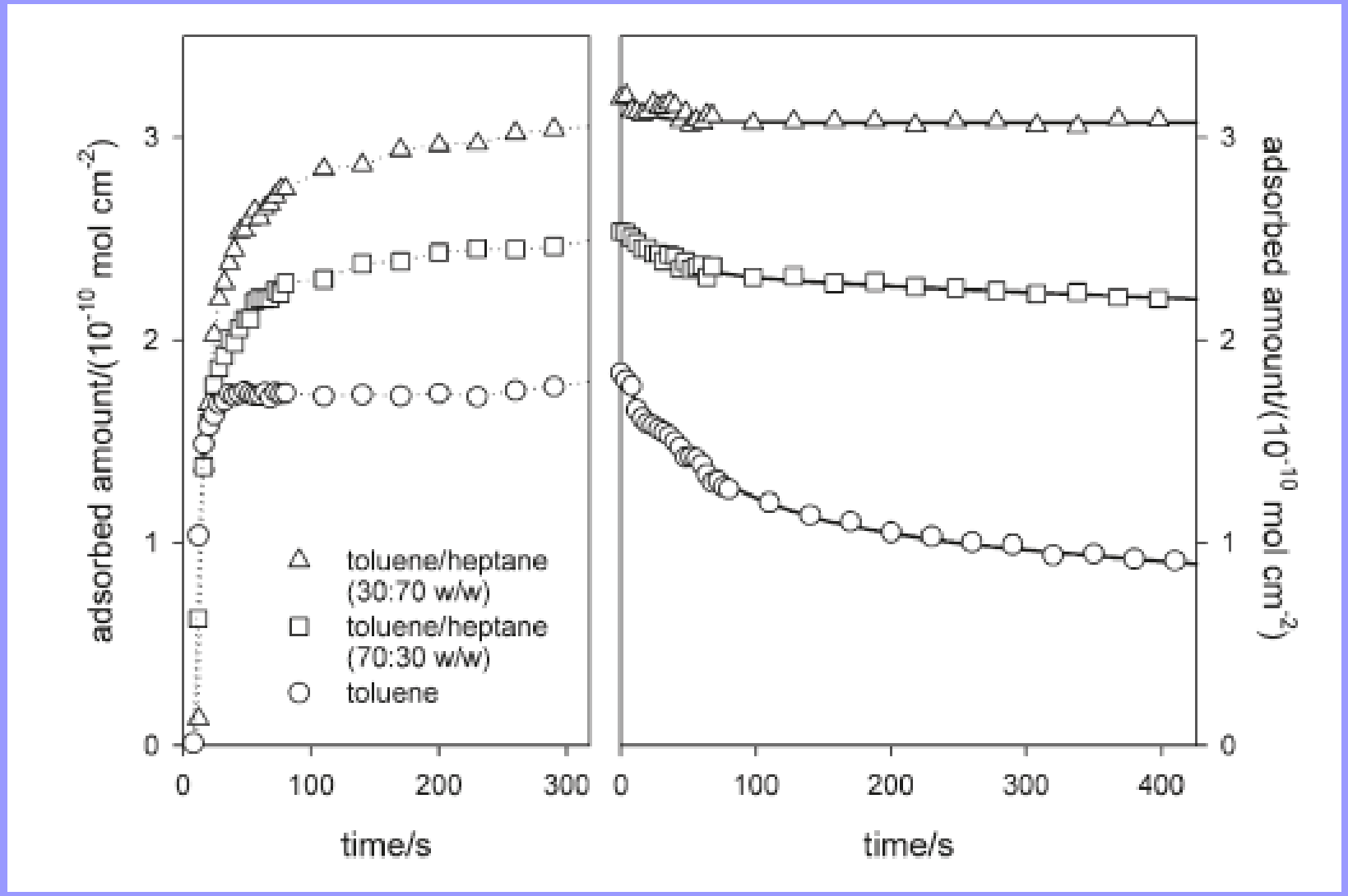

effects of trace moisture

non-ionic surfactants

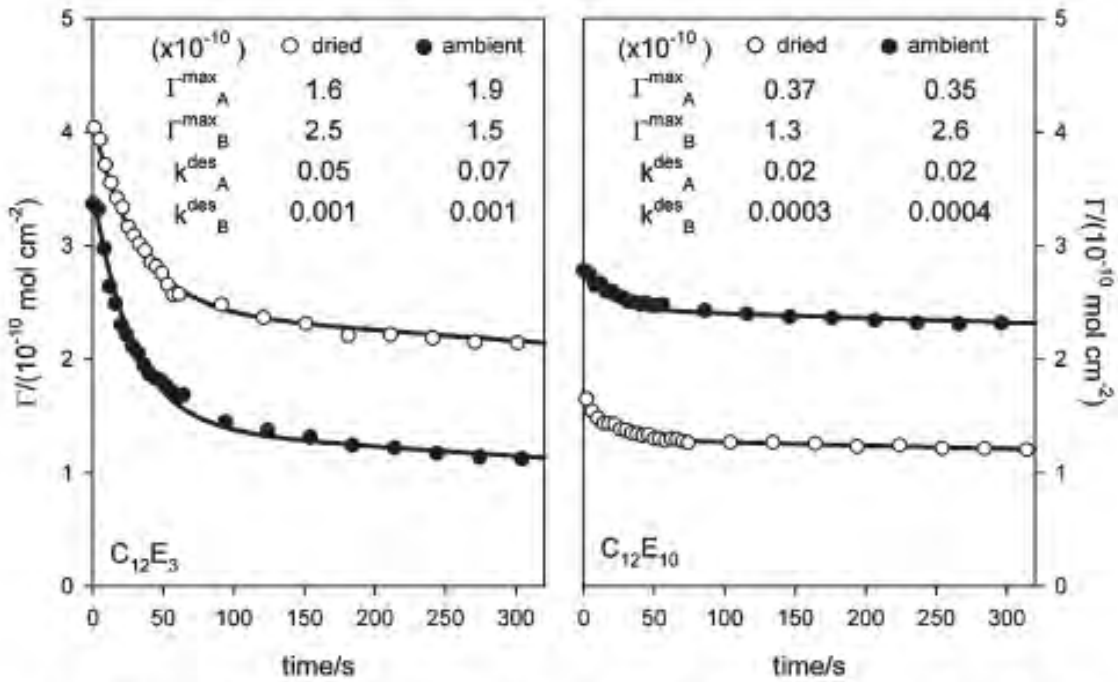

Figure 10. Comparison of desorption rates for $C_{12}E_3$ and $C_{12}E_{10}$ from ambient and dried toluene. Solid lines are fits to the data generated as described in the text. The units of $\Gamma^{max}_{A,B}$ are mol cm^{-2}; $k^{des}_{A,B}$ have units of mol cm^{-2} s^{-1}. Characteristic errors are $\Gamma^{max}_{A,B} \pm 0.1 \times 10^{-10}$ mol cm^{-2}, $k^{des}_{A} \pm 0.02 \times 10^{-10}$ mol cm^{-2} s^{-1}, and $k^{des}_{B} \pm 0.0001 \times 10^{-10}$ mol cm^{-2} s^{-1}. Units are chosen to retain a constant prefactor and remain consistent with previous plots.

effects of trace moisture

di-alkyl cationics

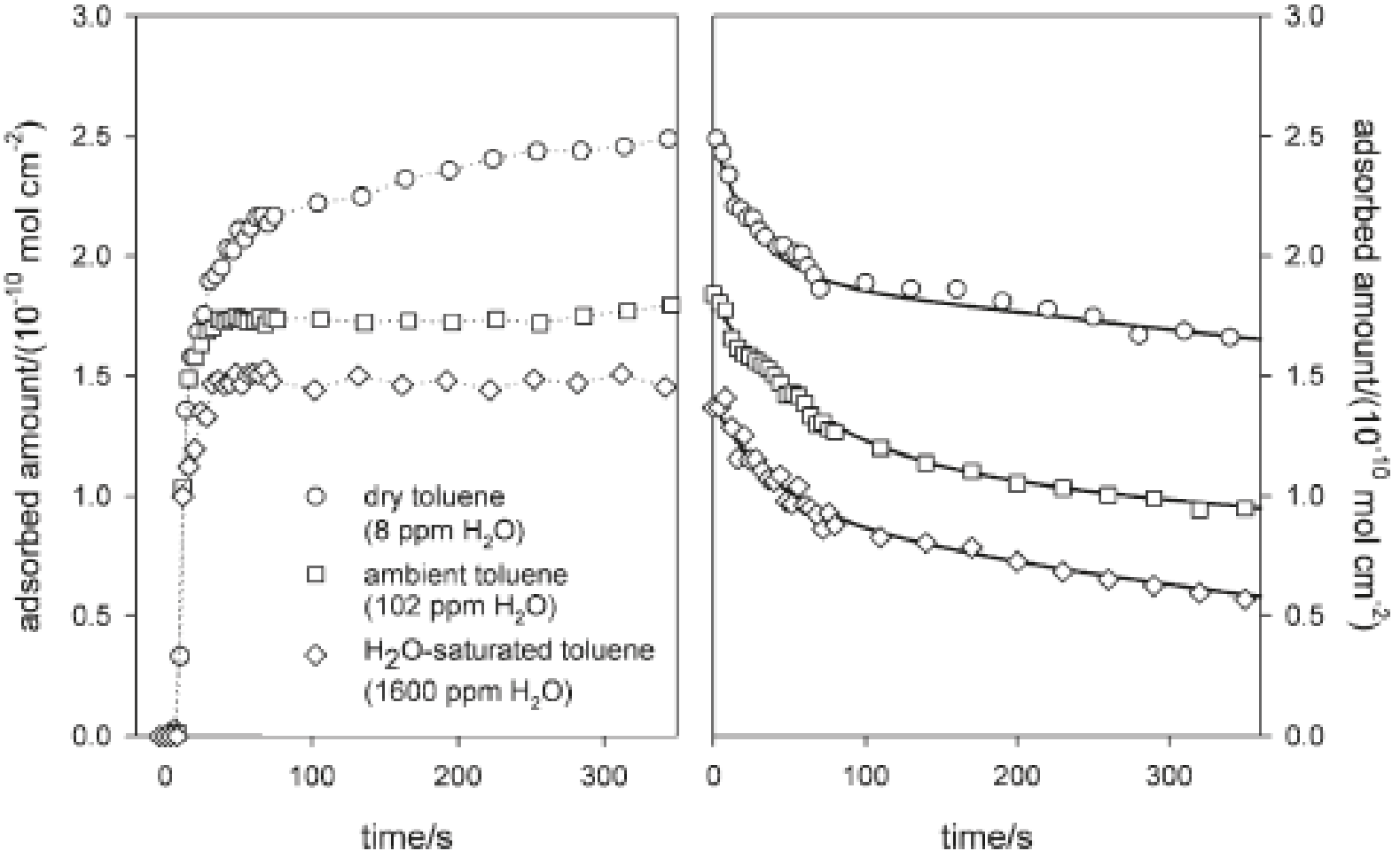

competing interactions

mechanistic diversity

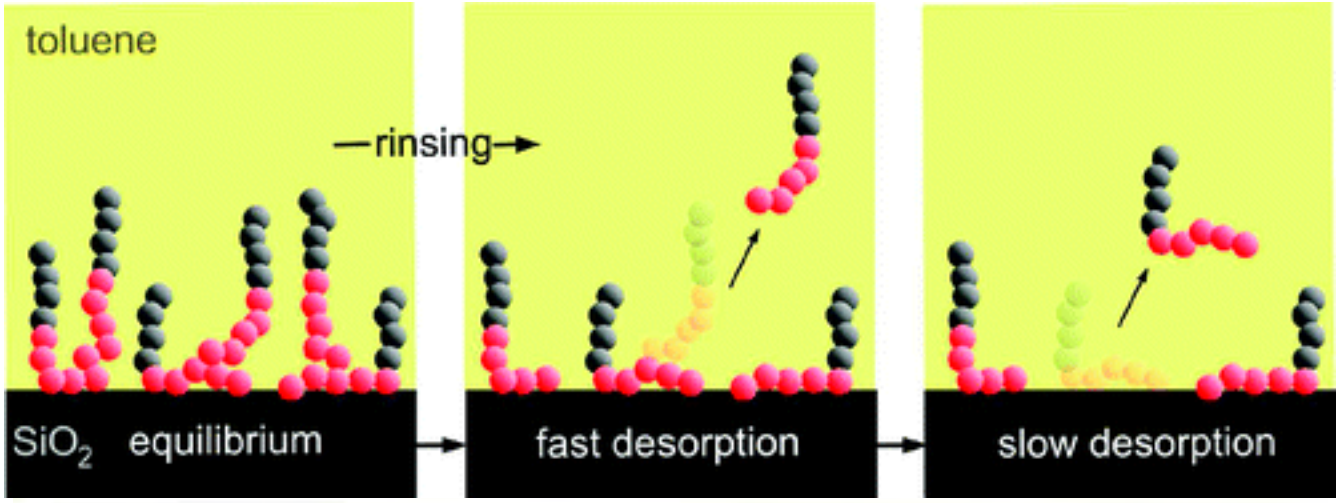

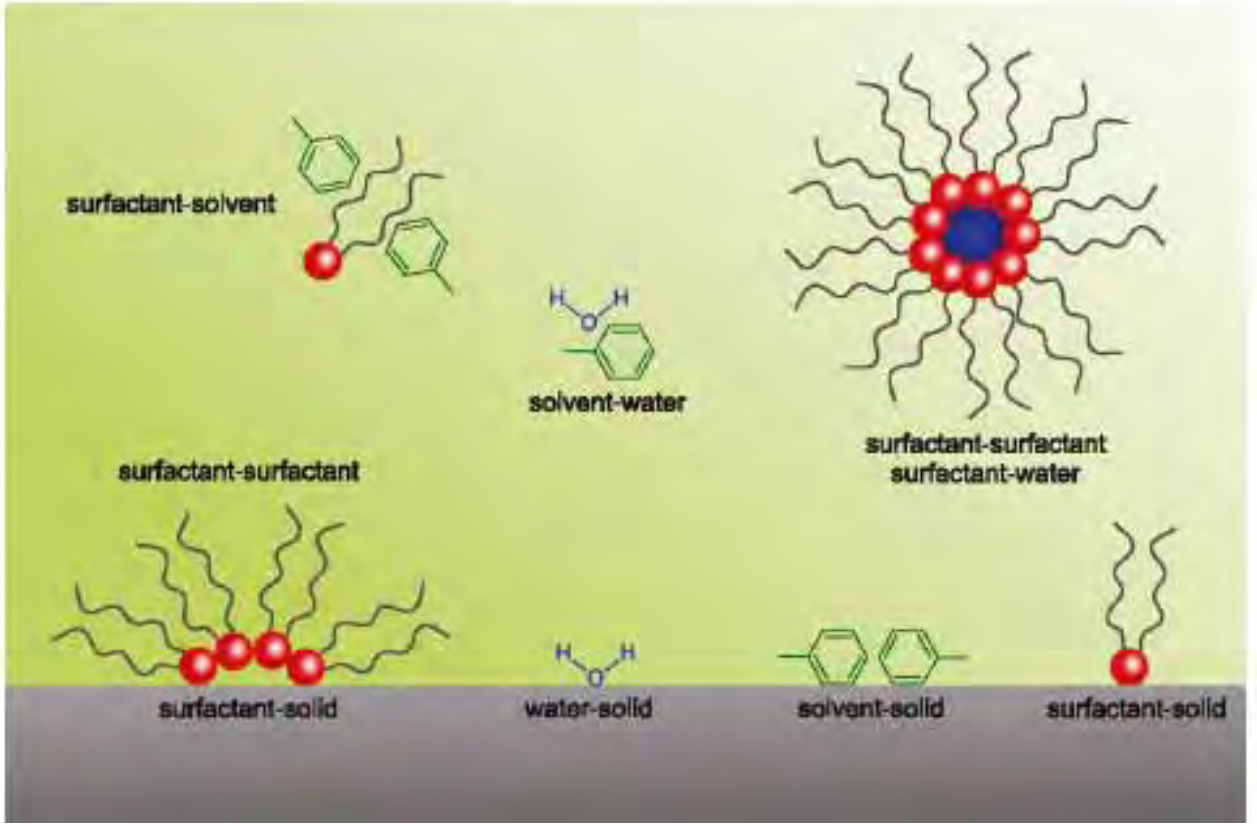

model inorganic colloids

dispersion structure

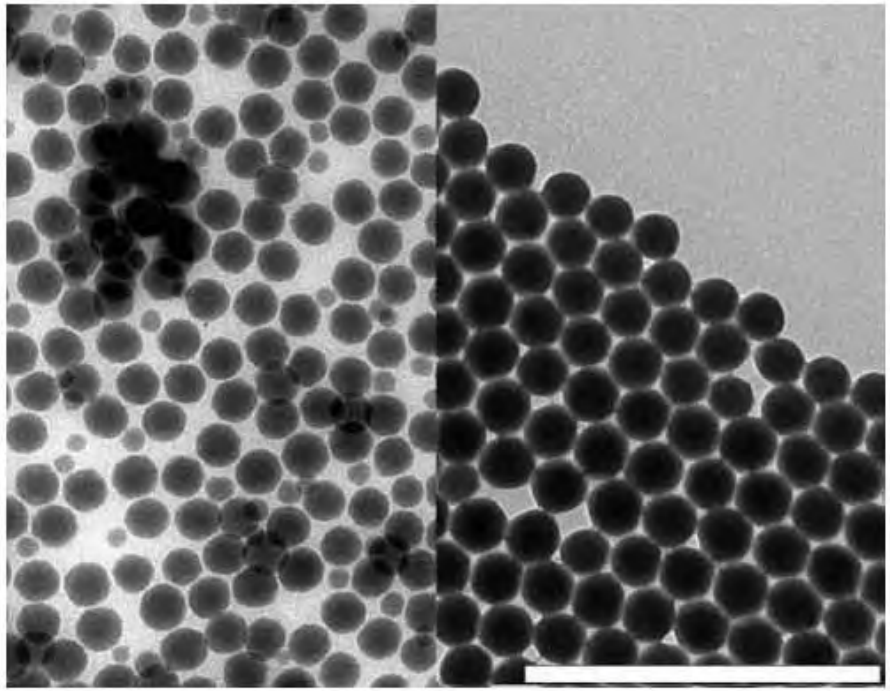

Figure 1. TEM images of 30CAL50 silica nanoparticles (starting conc 4 wt %) dried with no added surfactant (left) and pretreated with 4 wt % AOT (right). The scale bar shown is 500 nm.

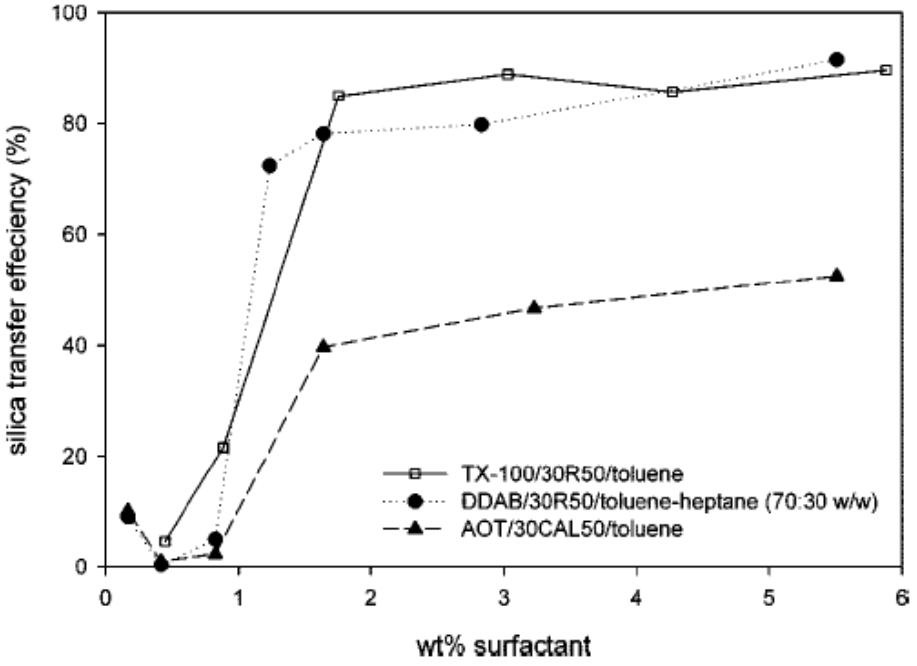

Formation of Surfactant-Stabilised Silica Organosols

Rico F. Tabor, Julian Eastoe, Peter J. Dowding
Isabelle Grillo and Richard K. Heenan

Langmuir, 2008, 24,12792-12797

model inorganic colloids in oil

dispersion structure

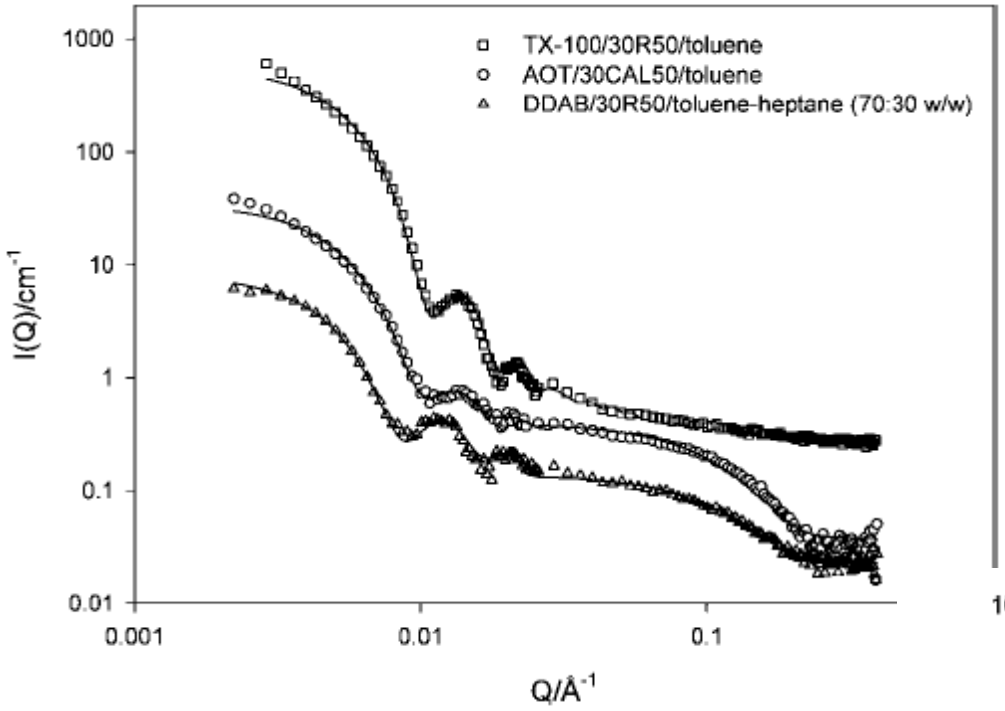

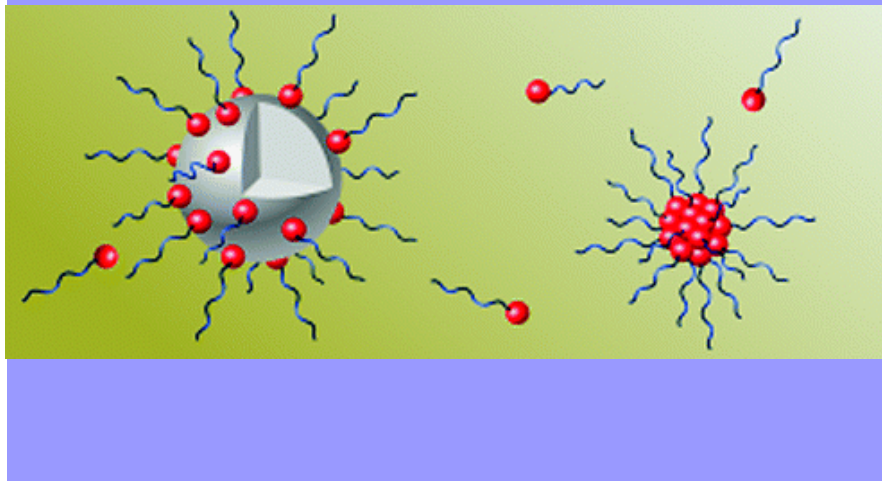

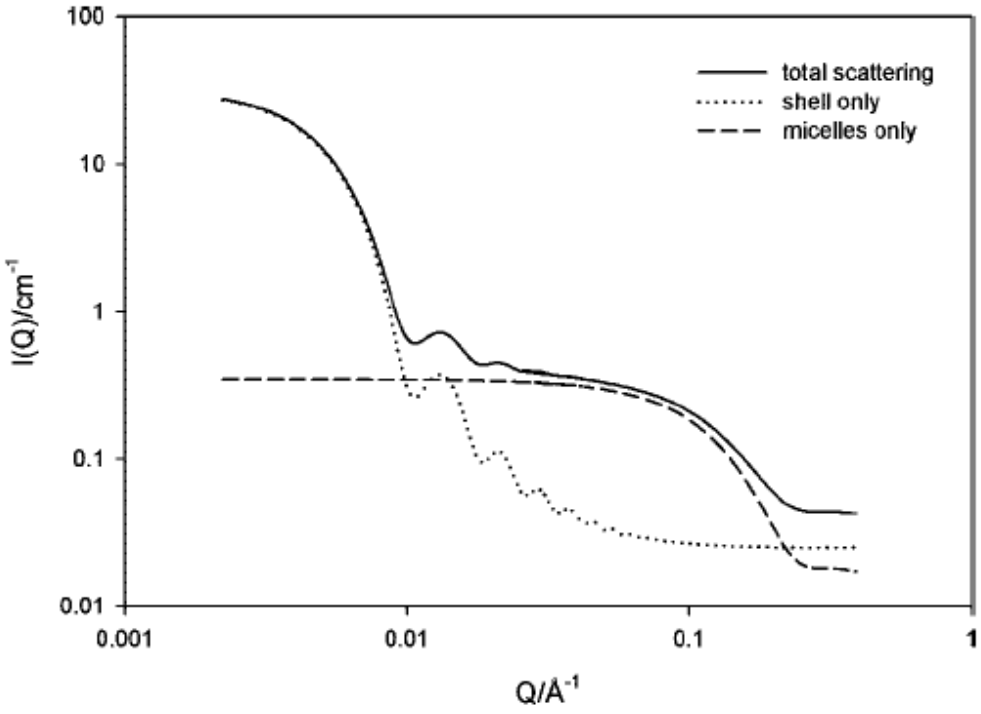

inorganic colloids + microemulsions

structure

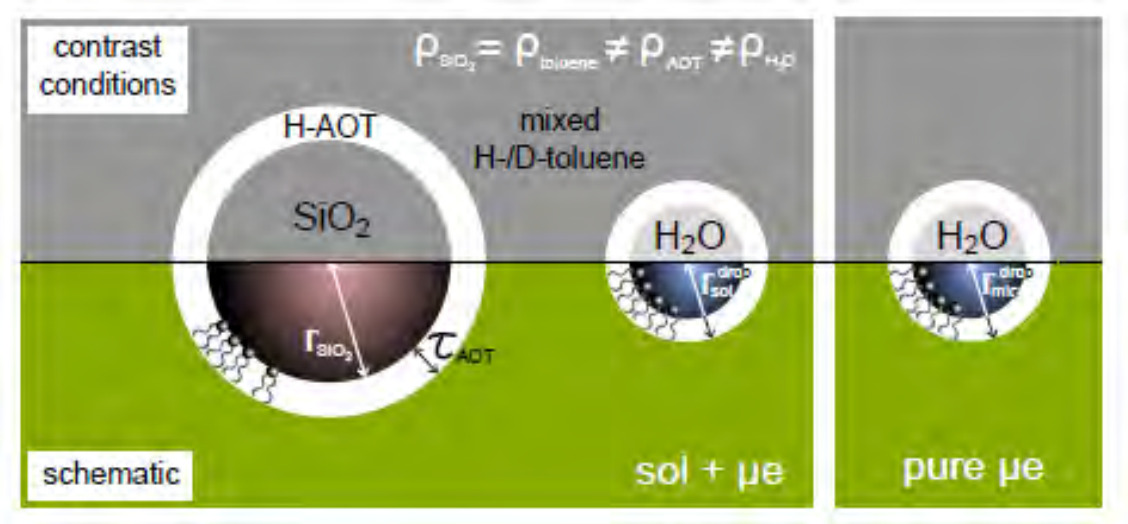

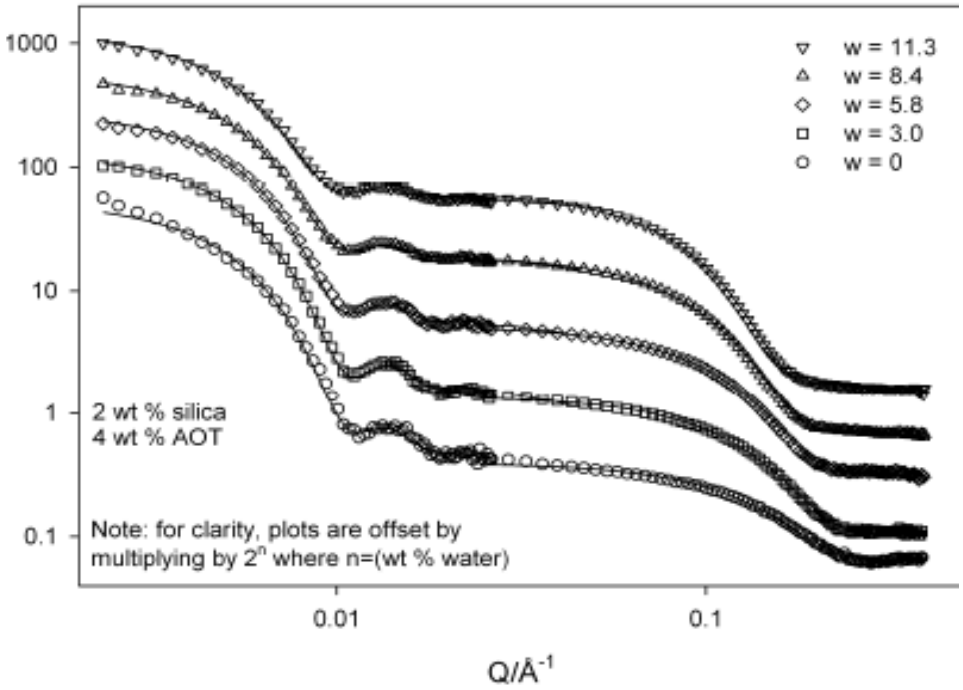

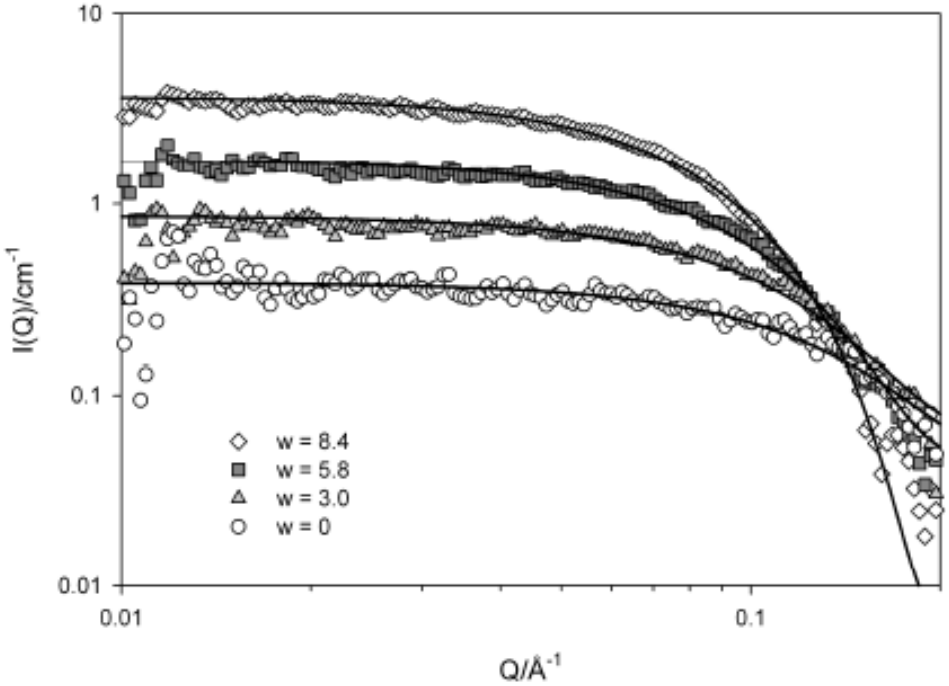

model inorganic colloids

stopped-flow SANS

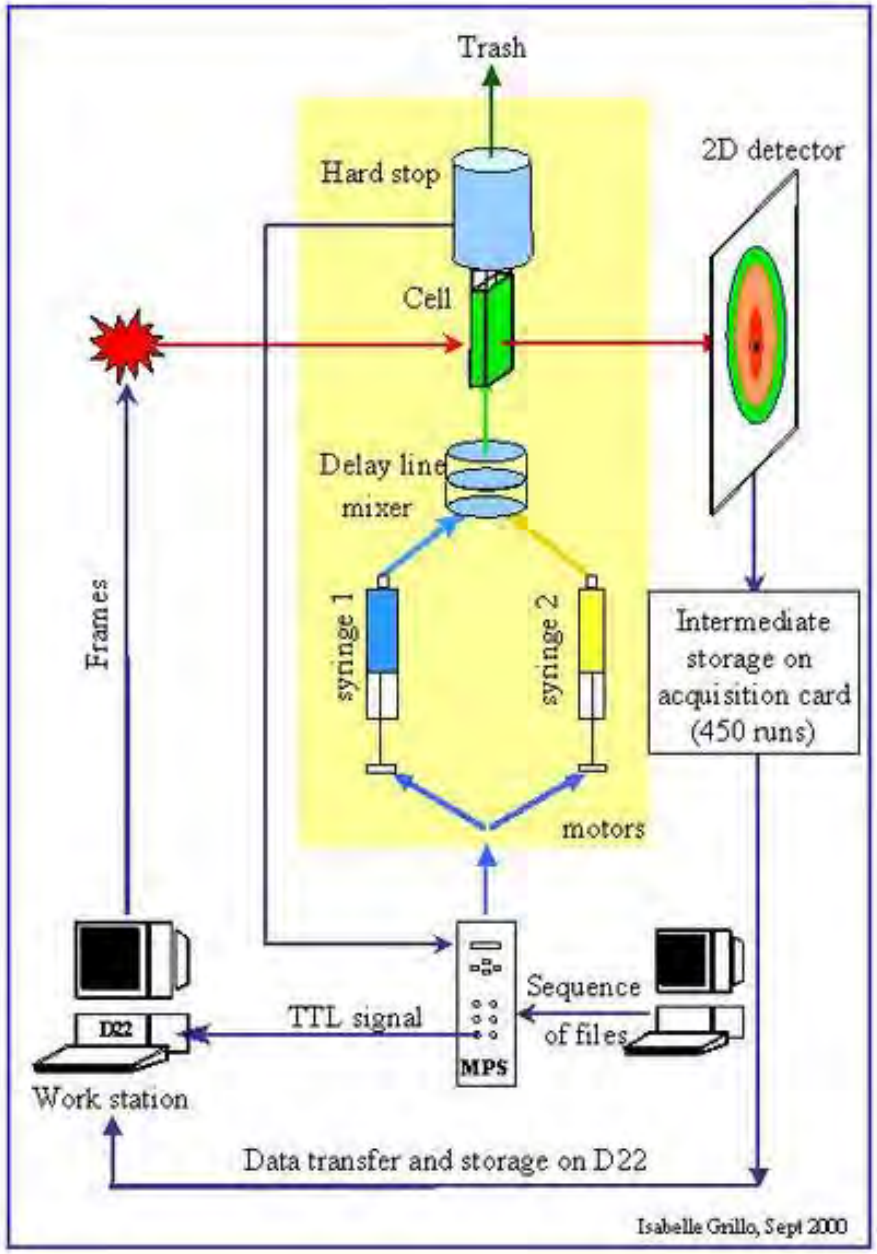

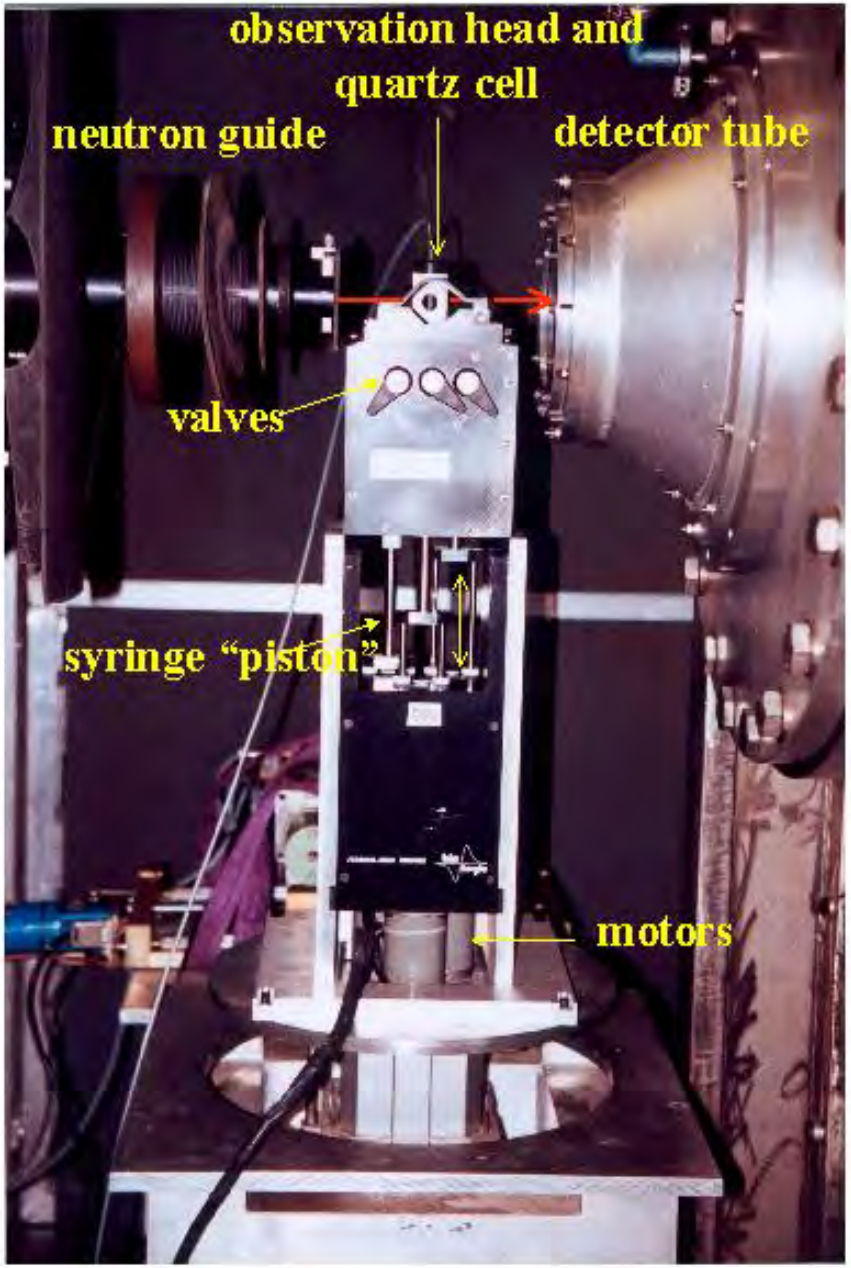

model inorganic colloids

stopped-flow SANS

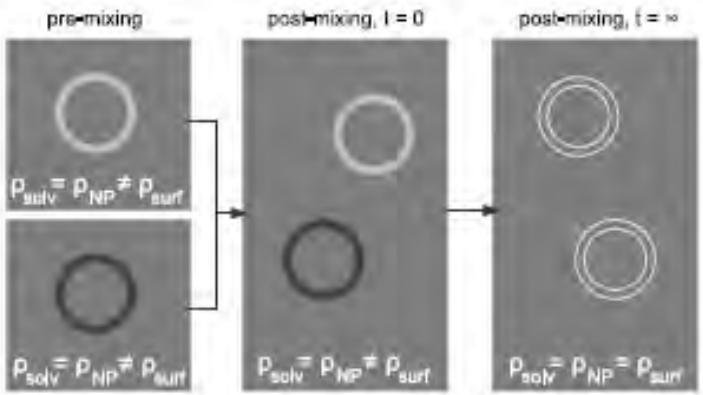

Figure 4.10: Schematic of the neutron contrast conditions used for the stopped-flow mixing experiment showing the effective scattering length densities of the nanoparticle (NP), surfactant (surf) and solvent (solv).

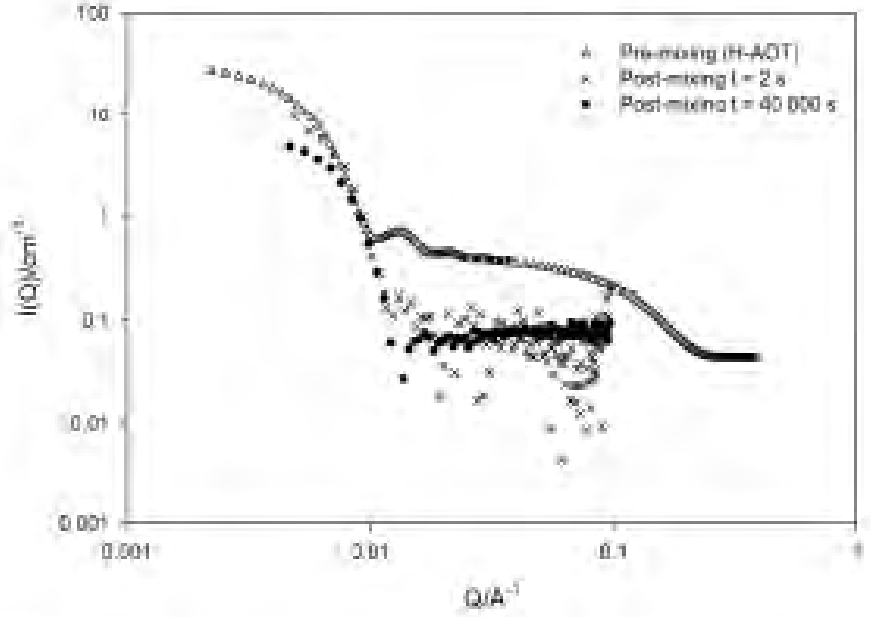

Figure 4.11: SANS data of a pre-mixing H-AOT stabilised sol showing shell (low-Q) and micellar (high-Q) scattering, and two post-mixing samples, which only show shell scattering.

model inorganic colloids

stopped-flow SANS

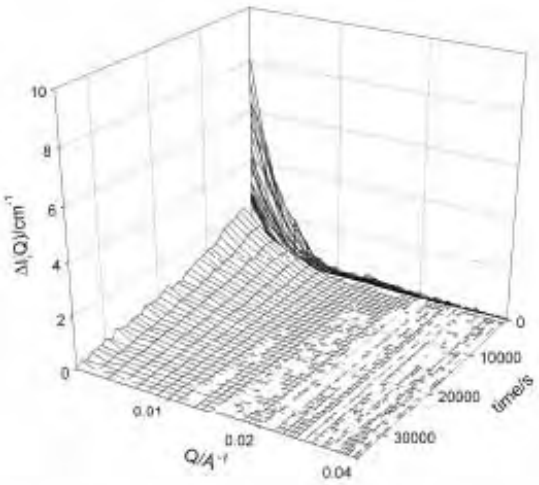

Figure 4.13: Time-resolved SANS data after the stopped-flow mixing of the stock sols, plotted as $\Delta I(Q)$, the difference between the spectra and the final time frame spectrum.

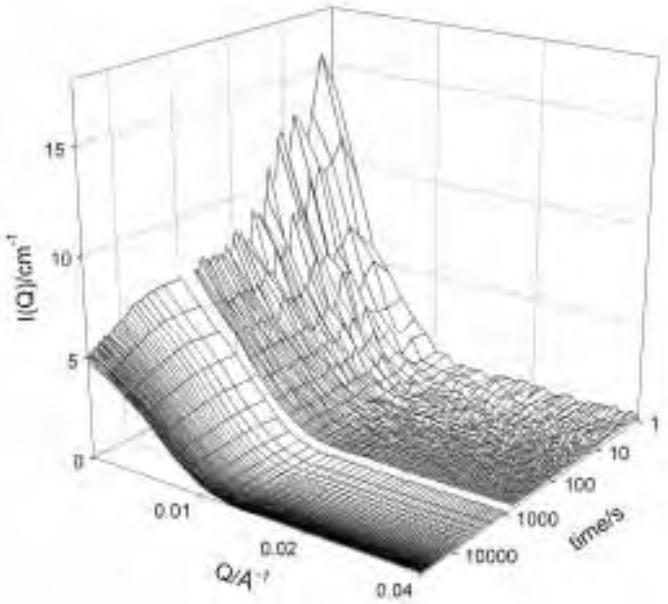

Figure 4.12: Time-resolved SANS data after the stopped-flow mixing of the stock sols. Note the logarithmic time scale to clearly show both the fast and slow processes.

acknowledgements

friends and colleagues

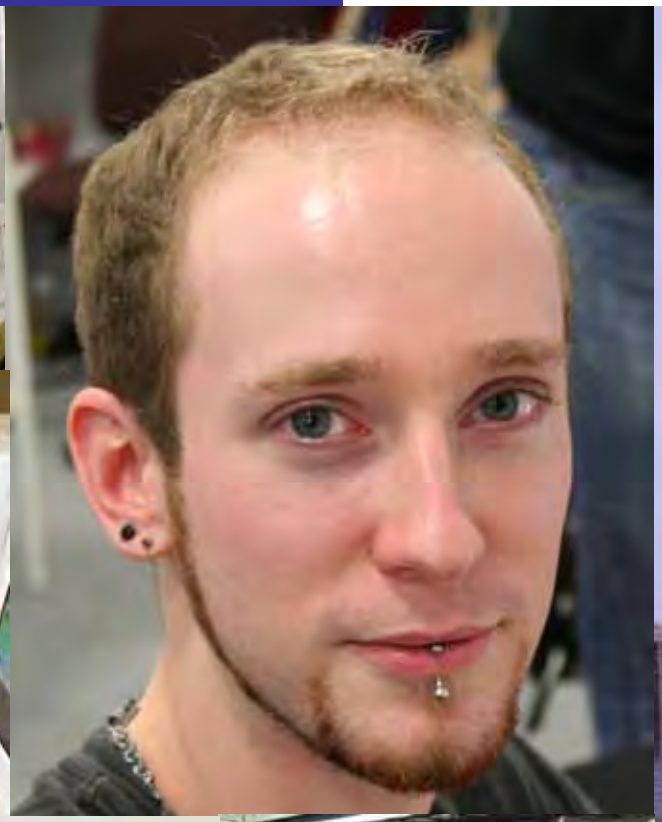

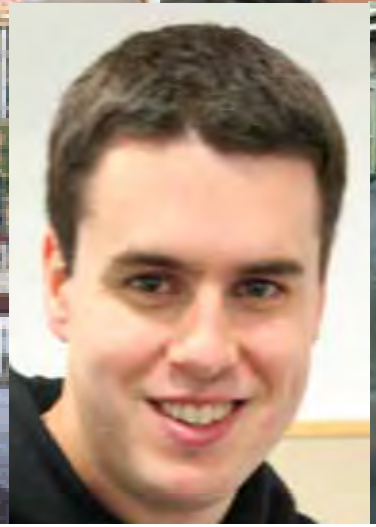


87091